



HAL
open science

Multidecadal Trends of the Mixed Layer Depth and Their Relation to the Wind in Global Ocean Models Forced by an Atmospheric Reanalysis

Anne-Marie Tréguier, Clement de Boyer Montégut, Steve Yeager, Eric Chassignet, Doroteaciro Iovino, Andrew E Kiss, Pengfei Lin, Camille Lique, Dmitry Sidorenko

► **To cite this version:**

Anne-Marie Tréguier, Clement de Boyer Montégut, Steve Yeager, Eric Chassignet, Doroteaciro Iovino, et al.. Multidecadal Trends of the Mixed Layer Depth and Their Relation to the Wind in Global Ocean Models Forced by an Atmospheric Reanalysis. *Journal of Geophysical Research. Oceans*, 2025, 130, <10.1029/2024JC022271>. <insu-05101551>

HAL Id: insu-05101551

<https://insu.hal.science/insu-05101551v1>

Submitted on 6 Jun 2025

HAL is a multi-disciplinary open access archive for the deposit and dissemination of scientific research documents, whether they are published or not. The documents may come from teaching and research institutions in France or abroad, or from public or private research centers.

L'archive ouverte pluridisciplinaire HAL, est destinée au dépôt et à la diffusion de documents scientifiques de niveau recherche, publiés ou non, émanant des établissements d'enseignement et de recherche français ou étrangers, des laboratoires publics ou privés.



Distributed under a Creative Commons CC BY-NC 4.0 - Attribution - Non-commercial use - International License

Multidecadal Trends of the Mixed Layer Depth and Their Relation to the Wind in Global Ocean Models Forced by an Atmospheric Reanalysis

**Key Points:**

- Multidecadal trends of the mixed layer depth in summer in Ocean Model Intercomparison Project (OMIP) models are related to trends in the wind speed used to force the models
- The increase of the summer mixed layer depth in the Southern Ocean from 1970 to 2018 is confirmed by the models
- Trends of the mixed layer depth are weaker in OMIP models than in observations, possibly due to an underestimation of the wind speed trends

Anne Marie Treguier¹ , Clément de Boyer Montégut¹ , Steve Yeager², Eric P. Chassignet³ , Doroteaciro Iovino⁴ , Andrew E. Kiss⁵ , Pengfei Lin⁶, Camille Lique¹ , and Dmitry Sidorenko⁷ 

¹University Brest, CNRS, Ifremer, IRD, Laboratoire d'Océanographie Physique et Spatiale (LOPS), IUEM, Brest, France, ²NSF National Center for Atmospheric Research, Boulder, CO, USA, ³Center for Ocean-Atmospheric Prediction Studies, Florida State University, Tallahassee, FL, USA, ⁴CMCC Fondazione—Euro-Mediterranean Center on Climate Change, Bologna, Italy, ⁵Research School of Earth Sciences and ARC Centre of Excellence for Climate Extremes, Australian National University, Canberra, ACT, Australia, ⁶State Key Laboratory of Numerical Modeling for Atmospheric Sciences and Geophysical Fluid Dynamics, Institute of Atmospheric Physics, Chinese Academy of Sciences, Beijing, China, ⁷Alfred Wegener Institute, Helmholtz Centre for Polar and Marine Research (AWI), Bremerhaven, Germany

Supporting Information:

Supporting Information may be found in the online version of this article.

Correspondence to:

A. M. Treguier,
anne-marie.treguier@univ-brest.fr

Citation:

Treguier, A. M., de Boyer Montégut, C., Yeager, S., Chassignet, E. P., Iovino, D., Kiss, A. E., et al. (2025). Multidecadal trends of the mixed layer depth and their relation to the wind in global ocean models forced by an atmospheric reanalysis. *Journal of Geophysical Research: Oceans*, 130, e2024JC022271. <https://doi.org/10.1029/2024JC022271>

Received 19 DEC 2024

Accepted 27 APR 2025

Author Contributions:

Conceptualization: Anne Marie Treguier, Clément de Boyer Montégut
Investigation: Anne Marie Treguier
Resources: Steve Yeager, Eric P. Chassignet, Doroteaciro Iovino, Andrew E. Kiss, Pengfei Lin, Dmitry Sidorenko
Validation: Clément de Boyer Montégut
Writing – original draft: Anne Marie Treguier
Writing – review & editing: Anne Marie Treguier, Clément de Boyer Montégut, Steve Yeager, Eric

Abstract The surface mixed layer of the ocean plays a key role in ocean-atmosphere interactions. Despite the ocean surface warming in the past four decades, which increased the stratification, the mixed layer depth (MLD) has been found to increase, most notably in the Southern Ocean in summer. We use 12 models from the Ocean Model Intercomparison Project (OMIP) at different resolutions, forced by the atmospheric reanalysis JRA55-do, to assess their capability to represent the MLD trends over the period 1970–2018 and to investigate their origin. The MLD evolution in the OMIP models is extremely well correlated across models at interannual time scales, especially in summer. Correlations are lower in high resolution models because of the chaotic nature of the mesoscale variability. OMIP models reproduce consistently the deepening trend of the mixed layer in summer in the Southern Ocean and confirm its relation to the wind speed. The MLD deepening is weaker in the models than in observations, probably due to the fact that the wind speed trend is underestimated in the atmospheric reanalysis. We find however that the MLD deepening is not a simple one-dimensional response to the increase of the wind speed at a given location, but that the three-dimensional processes that control the stratification also play a part. This study gives confidence in the capacity of ocean models to project the response of the mixed layer to future changes in wind speed.

Plain Language Summary The top layer of the ocean mediates the transfers of heat and gases between the atmosphere and the deep ocean. It is called the mixed layer because it is homogenized vertically by turbulent processes. Changes in the thickness of this layer have been observed over the past decades, and are expected in the future due to anthropogenic climate change. It is thus very important to understand the drivers of the observed changes and to assess whether the ocean-ice models used for climate projections can represent the relevant processes. We consider 12 models forced by the same atmospheric forcing over the period 1970–2018 and we find that they reproduce the mixed layer deepening observed in the Southern Ocean in summer. In the most realistic models, ocean eddies generate interannual variability of the mixed layer in energetic regions such as the Gulf Stream or Kuroshio, obscuring the long-term trends. The models confirm that the mixed layer deepening is related to the increase in wind speed over the Southern Ocean in the past decades. The increase in wind speed strengthens the turbulent mixing locally, but changes in the ocean circulation below the mixed layer also play a part in the long-term trends.

1. Introduction

The ocean has absorbed about 90% of the energy accumulated in the earth system due to the human-induced increase in greenhouse gases in the atmosphere (Gulev et al., 2021; von Schuckmann et al., 2020), with the upper ocean warming faster than the deep ocean. This results in an increase of the upper ocean stratification (Yamaguchi & Suga, 2019). This stratification is not uniform vertically: the layer of maximum vertical density gradient, the upper ocean pycnocline (Sérazin et al., 2023), is overlaid by a well-mixed layer where the stratification is very low due to mixing by surface waves, Langmuir cells, shear-driven turbulence, and convection

© 2025 The Author(s).

This is an open access article under the terms of the [Creative Commons Attribution-NonCommercial License](https://creativecommons.org/licenses/by-nc/4.0/), which permits use, distribution and reproduction in any medium, provided the original work is properly cited and is not used for commercial purposes.

P. Chassignet, Doroteaciro Iovino, Andrew E. Kiss, Pengfei Lin, Camille Lique, Dmitry Sidorenko

(Belcher et al., 2012; D'Asaro, 2014). It has long been assumed that the increased stratification would lead to a shallowing of the ocean mixed layer (Bindoff et al., 2019), because the stratification below the mixed layer acts as a barrier, reducing diffusivity and preventing mixed layer deepening, but this has been questioned by recent studies as reported by Fox-Kemper et al. (2021).

Somavilla et al. (2017) were the first to document mixed layer deepening trends from hydrographic time series in the subtropical North Atlantic and North Pacific over the period 1990–2015. The deepening trends were 4.3 m/decade and 6.8 m/decade, respectively. They found similar trends in ocean reanalyses at the location of the hydrographic stations. In the reanalyses, these trends were spatially coherent over large regions, but not of a uniform sign over an ocean basin, and dependent on changes in the water masses advected at depth. The winter trends were explained by changes in the buoyancy forcing (densification of the surface waters favoring convection) but also an increased downward Ekman pumping. Sallée et al. (2021, hereafter S21) further analyzed upper ocean trends using a global data set of hydrographic observations over a longer period (1970–2018). They confirmed the increase in stratification documented by Yamaguchi and Suga (2019) due to warming, but also to freshening in the Southern Ocean and in the intertropical convergence zones. S21 found that despite this increase in stratification, the summer mixed layer depth was increasing by 2.9 m/decade almost globally, the trend reaching 10 m/decade in the Southern Ocean, supporting Fox-Kemper et al. (2021). Deepening trends were also found in winter, but they were less significant. S21 reviewed the processes that could induce a deepening of the mixed layer despite the surface warming and strengthening of the upper ocean pycnocline, and pointed to surface-forced mechanical turbulence. Noting that the wind speed over the ocean has been increasing (Young & Ribal, 2019), they examined the different mechanisms through which a wind speed increase could deepen the mixed layer, despite a strengthening stratification. They argued that mixing due to Langmuir circulation, sub-mesoscale frontal instabilities and instabilities of wind-driven inertial oscillations and internal wave shears could contribute to the observed deepening, the latter being the most likely candidate.

Whether the mixed layer will deepen or shallow in the future is an important issue, because its thickness influences air-sea exchanges (Rudzin et al., 2018) and primary production (Llort et al., 2019). The coupled ocean-atmosphere models participating in the Coupled Model Intercomparison Project tend to project shallower mixed layer depths in future scenarios (Alexander et al., 2018; Fox-Kemper et al., 2021; Sallée et al., 2013), but there is low confidence in these results because CMIP models have large biases in their representation of the mixed layer (Fox-Kemper et al., 2021, and references therein). Most climate models have a grid resolution of about 100 km and processes impacting the mixed layer are parameterized: vertical processes such as those examined by S21, as well as mesoscale processes that have been shown to structure the spatial variability of the mixed layer in observations and models (Gaubert et al., 2019; Treguier et al., 2023).

The Southern ocean, where multidecadal mixed layer trends were the largest in S21, is characterized by a high level of mesoscale eddy energy, which makes high resolution models necessary for the evaluation of trends over the historical period. Li and Lee (2017) used the POP model at 1/10° resolution to analyze the seasonal deepening of the mixed layer at the equatorward edge of the subantarctic front, south of Australia. They demonstrated the role of buoyancy advection by a jet-scale overturning circulation, which was driven by the eddy momentum fluxes that intensify the jet. Using a regional coupled model at 9 km resolution, Gao et al. (2023) demonstrated that buoyancy advection plays a major role in the mixed layer variability at the mesoscale, especially in winter when the MLD is larger. Thus, ocean mesoscale dynamics influence the evolution of the MLD on seasonal time scales, but their possible influence on longer time scales has not been considered, nor their possible contribution to the trends revealed by S21.

The objective of our study is to assess the capability of current global ocean models to represent the observed multi-decadal trends of the mixed layer depth and their relation to the winds. For this purpose, we use models that participate in the Ocean Model Intercomparison Project (OMIP, Griffies et al., 2016). We consider models with resolutions of 1/10° or finer, representing mesoscale dynamics, and compare them with lower resolution versions representative of the CMIP models (about 1°). The improvements brought by the higher resolution in OMIP models have been documented by Chassignet et al. (2020) and Treguier et al. (2023). The analysis of mixed layer biases in OMIP shows that they are similar in amplitude to those of the CMIP models (Tsujino et al., 2020), and that these biases are model dependent as well as resolution dependent (Treguier et al., 2023).

In this paper, we address the following questions. (a) Although different models have different mixed layer biases, are their interannual variability and trends similar, when forced by the same atmospheric forcing? (b) Do the

Table 1
Characteristics of the OMIP Models Used in This Study

Model	Horizontal grid for the model pairs	Mixed layer vertical mixing parameterizations
ACCESS-MOM (Kiss et al., 2020)	1° tripolar	KPP, FFH
	1/10° tripolar	KPP, FFH
AWI-FESOM (Sein et al., 2018)	Unstructured 1°	KPP
	Unstructured 10–50 km	
IAP-LICOM (L. Li et al., 2020)	1° tripolar	Canuto MLD scheme
	1/10° tripolar	
NCAR-POP (Danabasoglu et al., 2020)	1° tripolar	KPP, FFH, Langmuir
	1/10° tripolar	KPP
FSU-HYCOM (Chassignet et al., 2020)	0.72° tripolar	KPP
	1/12° tripolar	
CMCC-NEMO (Iovino et al., 2016)	1° tripolar	TKE
	1/16° tripolar	

Note. Consortia or institution names are as follows: Australian Community Climate and Earth System Simulator (ACCESS), Alfred Wegener Institute (AWI), Florida State University (FSU), Institute of Atmospheric Physics (IAP), National Center for Atmospheric Research (NCAR), Centro Euro-Mediterraneo sui Cambiamenti Climatici (CMCC). The ocean models are based on the Modular Ocean Model (MOM, Griffies, 2012; Kiss et al., 2020), the Finite element/volume Sea ice-Ocean Model (FESOM, Wang et al., 2014), the LASG/IAP Climate system Ocean Model (LICOM, L. Li et al., 2020; Lin et al., 2020), the Parallel Ocean Program (POP, Smith et al., 2010), the HYbrid Coordinate Ocean Model (HYCOM, Chassignet et al., 2003) and the Nucleus for European Modeling of the Ocean (NEMO, Madec & the NEMO team, 2016). The mixed layer parameterizations are the K-profile parameterization (KPP, Large et al., 1994); the Turbulent Kinetic Energy (TKE, Blanke & Delecluse, 1993), the parameterization of submesoscale eddy effects (FFH, Fox-Kemper et al., 2008), Langmuir (Q. Li et al., 2016) and the Canuto scheme (Canuto et al., 2001, 2002). For all model pairs except NCAR-POP, the mixing schemes are the same at low and high resolution.

OMIP models reproduce the deepening trend of the mixed layer diagnosed by S21 in summer? (c) Do the OMIP models confirm the relations between mixed layer depth trends and wind trends hypothesized by S21?

2. Models

OMIP ocean-ice models are forced by the same atmospheric state: for OMIP2, the forcing is JRA55-do, derived from the Japanese 55 years reanalysis (Griffies et al., 2016; Tsujino et al., 2018). The forcing covers the period 1958–2018. The OMIP protocol advises repeating this forcing cycle 6 times to allow a better spin-up of the ocean state. However, only one cycle has been run for most high resolution models, because of the high cost of these simulations. As a consequence, we use only the first OMIP cycle for both low and high resolution models. This is adequate for the present study because spin-up effects are expected to affect deep water masses and not so much the surface ocean, which largely equilibrates after a few seasonal cycles. Following Treguier et al. (2023, hereafter T23), we select all the available high resolution OMIP2 models and their low resolution counterparts (6 model pairs, listed in Table 1). The high resolution models are selected because they explicitly represent the mesoscale dynamics, excepted in polar regions and on continental shelves (Hallberg, 2013). We also evaluate the low resolution models because this class of models is commonly used for climate projections. The description of each model can be found in T23 and in Chassignet et al. (2020), and is not repeated here.

The mixed layer depth (MLD) is computed using the threshold method proposed by Griffies et al. (2016) and also used by S21, with a uniform density threshold of 0.03 kg.m^{-3} and a reference level of 10 m. However, not all OMIP models used this approach for their online MLD computations. Moreover, the threshold has often been computed relative to the density at the top model level, the depth of which varies across models (T23), and is different from the 10 m level used in observation data sets (de Boyer Montégut et al., 2004; Holte et al., 2017). T23 showed that it is necessary to use a common reference level for a proper comparison of the MLD between models and for the evaluation of the models using observations. For these reasons, T23 recomputed the MLD in all models using a 10 m reference level and a uniform density threshold of 0.03 kg.m^{-3} . This had to be performed using monthly mean temperature and salinity model outputs, because unfortunately daily outputs were not available for all models and for the whole duration of the simulations. We acknowledge that MLDs computed from monthly versus daily archives differ, because submonthly variance can create significant rectified effects as

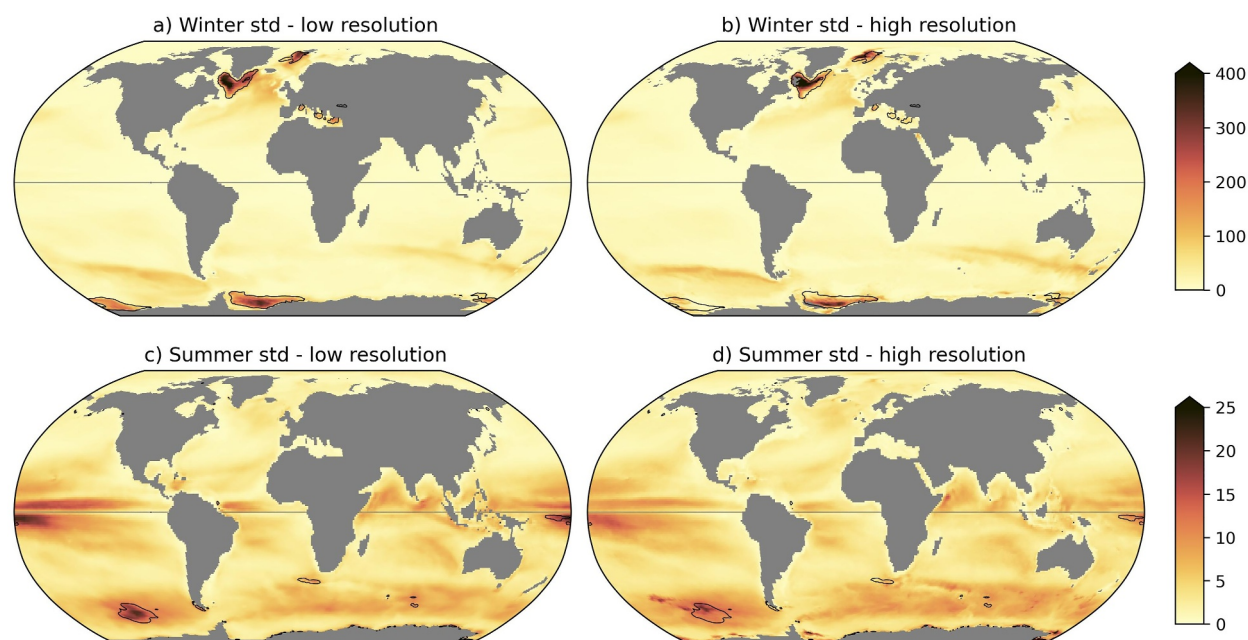


Figure 1. Multi-model mean of the interannual standard deviation of the MLD [m] over 49 years (1970–2018). Black contours indicate regions where the inter-model standard deviation exceeds 100 m (winter) or 5 m (summer). The winter (summer) season is the average over the months of January to March in the Northern (Southern) Hemisphere, and July to September in the Southern (Northern) Hemisphere, respectively.

documented by T23 (their Figure 6), especially during the Northern Hemisphere spring. However, T23 also found that inter-model differences are larger than the differences induced by different sampling frequencies. Using 12 models gives us confidence in the robustness of our analysis.

The modeled MLDs are first computed on the native grids of the models, but our focus is on interannual variability and trends at spatial scales larger than 100 km. In order to consider similar spatial scales in low and high resolution models, we process the MLD following the approach in T23. The high resolution MLDs are coarsened through spatial averaging toward a nominal 1° grid (coarsening by a factor of 10 for IAP-LICOM, ACCESS-MOM and NCAR-POP, a factor of 12 for FSU-HYCOM and 16 for CMCC-NEMO, using the `.coarsen().mean()` function from xarray). To facilitate validation and inter-comparisons, both model and observation MLDs are then regridded by bilinear interpolation to a common grid with a nominal resolution of 1°. We choose a Mercator grid due to its quasi-isotropy at polar latitudes; this type of grid is often used in observation products or models (Gaillard et al., 2016; Willebrand et al., 2001). Coarsening and regridding are performed prior to the computation of statistics and trends. As T23 and S21, we focus on two seasons: the winter (summer) season, defined as the average over the months of January to March in the Northern (Southern) Hemisphere, and July to September in the Southern (Northern) Hemisphere, respectively.

3. Modeled Variability of the Mixed Layer Depth and Its Correlation Across Models

Before exploring multidecadal trends of the MLD, we consider in this section the interannual variability, because the physical mechanisms that may cause multidecadal trends (as discussed in the literature e.g., S21) should also influence the MLD on interannual time scales. One cycle of the OMIP forcing simulates only one multidecadal trend over the 1970–2018 period, while the interannual variability is described with more degrees of freedom over the same period and therefore should be quite robust across models.

To set the stage, let us consider global maps of the interannual standard deviation of MLD in the models. The multi-model mean is shown in Figure 1 for conciseness, but inter-model differences are large in regions of high variability (contours in Figure 1). Maps for individual models are found in Figures S1–S4 in Supporting Information S1. In winter (Figures 1a and 1b), the interannual variability of the mixed layer is larger where the mean mixed layer is deep (see T23, Figure 1). The hot spots of interannual variability are the subpolar North Atlantic (Labrador and Irminger seas) and the Nordic seas, as well as the Antarctic Circumpolar Current (ACC). The

Weddell Sea is also a region of large interannual variability in the OMIP models, but this reflects biases of some of the models (Figures S1 and S3 in Supporting Information S1). For example, at low resolution, the FSU-HYCOM and ACCESS-MOM models have excessively deep mixed layers in the Weddell Sea in winter (biases larger than 3,000 m, see T23) and this is reflected in the multi-model mean interannual variability (Figure 1a). This is consistent with the CMIP6 multi-model mean (Heuzé, 2021) which shows biases exceeding 1000 m in the Weddell Sea. At high resolution, this bias is reduced in FSU-HYCOM, but increased in IAP-LICOM (T23, Figure 7). A hot spot of interannual variability is also found in the Nordic seas. T23 noted that the location of the deep mixed layers in the Greenland Sea were more accurately represented by the high resolution models, while some low resolution models had excessively deep mixed layers in the Norwegian sea.

Overall, just as was the case for the mean MLD (T23), the inter-model differences in MLD interannual standard deviation are larger than the differences between resolutions within each model pair (Figures S1 and S3 in Supporting Information S1).

In the summer season, the mixed layer is shallower and its interannual variability is reduced accordingly (note the different color scale for Figures 1c and 1d; Figures S2 and S4 in Supporting Information S1). Interannual variability is large in the tropics and in the Southern Ocean. We note that the variability is stronger at low resolution around 5°N, probably due to the deep bias diagnosed by T23, which is greatly reduced in high resolution models. In the ACC, the presence of resolved eddies at high resolution may increase the interannual variability in some regions, for example, downstream of the Agulhas retroflexion.

Despite models having different biases (T23), is the interannual variability of MLD robust across these models forced by the same atmospheric state? To answer this question, we have computed the 15 pair-wise Pearson correlation coefficients of all the pairs among the 6 low resolution models, the same for the 6 high resolution models, and the 6 correlations between the low resolution and high resolution members of each model pair. The correlations are computed for the MLD averaged for each winter or summer, over 49 years (1970–2018 period). The mean and linear trends have been removed from all series before the computations. The average of all model pairs is shown in Figure 2 for winter and summer (correlations for each pair are found in the Supporting Information S1, Figures S5–S10 in Supporting Information S1). The high positive correlation of the MLD series between the model pairs is striking, and extremely significant at the global scale for low resolution models in summer (Figure 2b). Clearly, the interannual variability of MLD in the models seems predominantly driven by their common atmospheric forcing. There are regions where the correlation across models is lower, especially in winter. These are regions of strong ocean dynamics such as the Gulf Stream and the boundary current of the North Atlantic subpolar gyre. In the low resolution models (Figure 2a), the different model biases (T23) result in different advection of water mass properties in these regions, thus leading to a different preconditioning of the water column in winter and a different MLD evolution at the interannual timescale. Inter-model correlations are clearly reduced at high resolution (Figures 2c and 2d) or when considering pairs of models at low and high resolution (Figures 2e and 2f), and are no longer significant in regions of high mesoscale turbulence: Gulf Stream, Kuroshio, ACC, Brazil-Malvinas confluence, Agulhas retroflexion, and, in winter, the western Bay of Bengal, the East Australian Current and the region west of Australia where eddies drift westwards. Mesoscale turbulence in the high resolution OMIP models is generated by the instabilities of the mean flow. Considering that the OMIP protocol does not include assimilation of ocean observations, mesoscale turbulence is not constrained directly by the interannual variability of atmospheric forcing, and it is expected to be uncorrelated between different models. It is well known that ocean mesoscales generate a so-called “intrinsic” variability at interannual time scales and large spatial scales (Penduff et al., 2018). T23 already pointed out that mesoscale eddies influence the spatial structure of the MLD in the OMIP models. Here we show that their presence decreases the inter-model correlations at high resolution compared with the low resolution models in mid-latitudes oceans. It is unclear whether eddies influence the correlations in polar regions in our models, because even the high resolution ones are not fully eddy-resolving in the polar oceans where the Rossby radius is small. Figure 2 shows that correlations are lower in the polar regions, at both high and low resolution, perhaps due to the added complexity arising from the presence of sea ice and its interaction with the surface layer. The correlations of individual pairs (Figures S5–S10 in Supporting Information S1) show a consistent behavior of all model pairs, except IAP-LICOM which has a lower correlation with the other five models. This may be related to this model having very specific biases, for example, a very shallow mixed layer in the Southern Ocean (T23), probably due to its use of a vertical mixing scheme unique among all the models (Table 1).

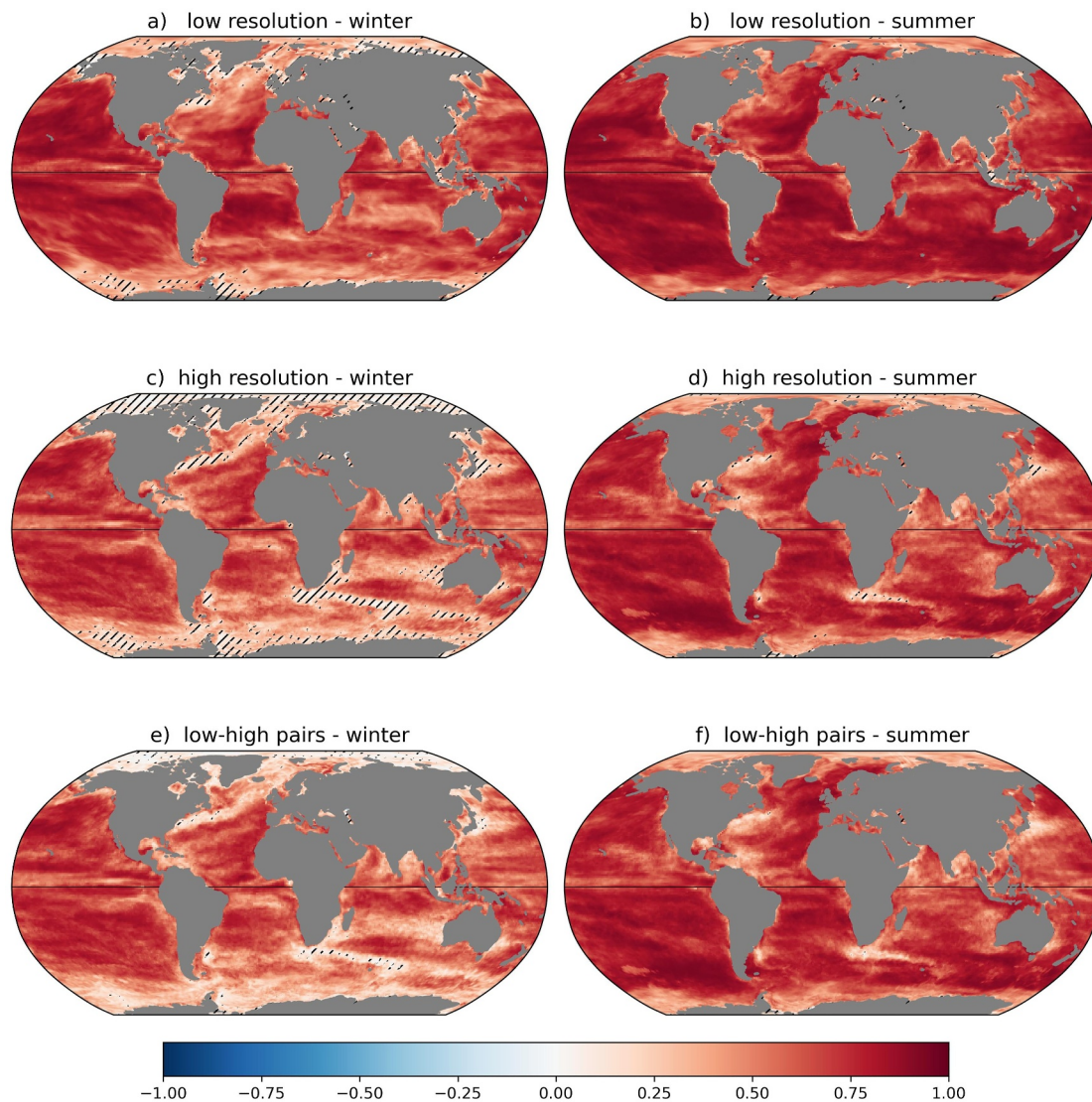


Figure 2. Pearson correlation coefficients for pairs of model time series of the MLD detrended interannual anomalies, 1970–2018. The correlation coefficient averaged between the 15 pairs of different low resolution models is shown in panels (a, b) for winter and summer respectively, and the average of the 15 pairs of high resolution models in panels (c, d). The average of the 6 correlations between the low resolution member and the high resolution member for each model pair from the same group is shown in panels (e, f). Regions where less than half the individual pair-wise correlations have a p -value lower than 0.1 are hatched (less than 8 members for panels a–d and less than 3 members for panels e–f). The winter (summer) season is the average over the months of January to March in the Northern (Southern) Hemisphere, and July to September in the Southern (Northern) Hemisphere, respectively.

Figure 2 demonstrates that the interannual variability of the MLD is largely driven by the atmosphere in OMIP models, but can the models shed some light on the processes involved? The surface buoyancy flux acts to restratify the ocean when positive (decreasing the MLD) and destratifies the ocean by convection when it is negative (thus increasing the MLD): these mechanisms would lead to a negative correlation between the buoyancy flux and the MLD. Vertical mixing processes, sensible heat loss and evaporation are enhanced when the wind is stronger, thus a positive correlation is expected between the MLD and the amplitude of the wind stress. However, the processes that govern the MLD are complex (Belcher et al., 2012; Somavilla et al., 2017). The MLD anomaly at a given location and year depends on the underlying stratification, which may have been modified by anomalous water mass properties or an anomalous ocean circulation, generated perhaps by atmospheric forcing, but at a different location and in a different year. These processes are often referred to as preconditioning (Gillard et al., 2022; Q. Li & Lee, 2017; Marshall & Schott, 1999). To exemplify the local relation between the MLD response and the air-sea fluxes, we have computed the times series of the surface buoyancy flux and wind stress

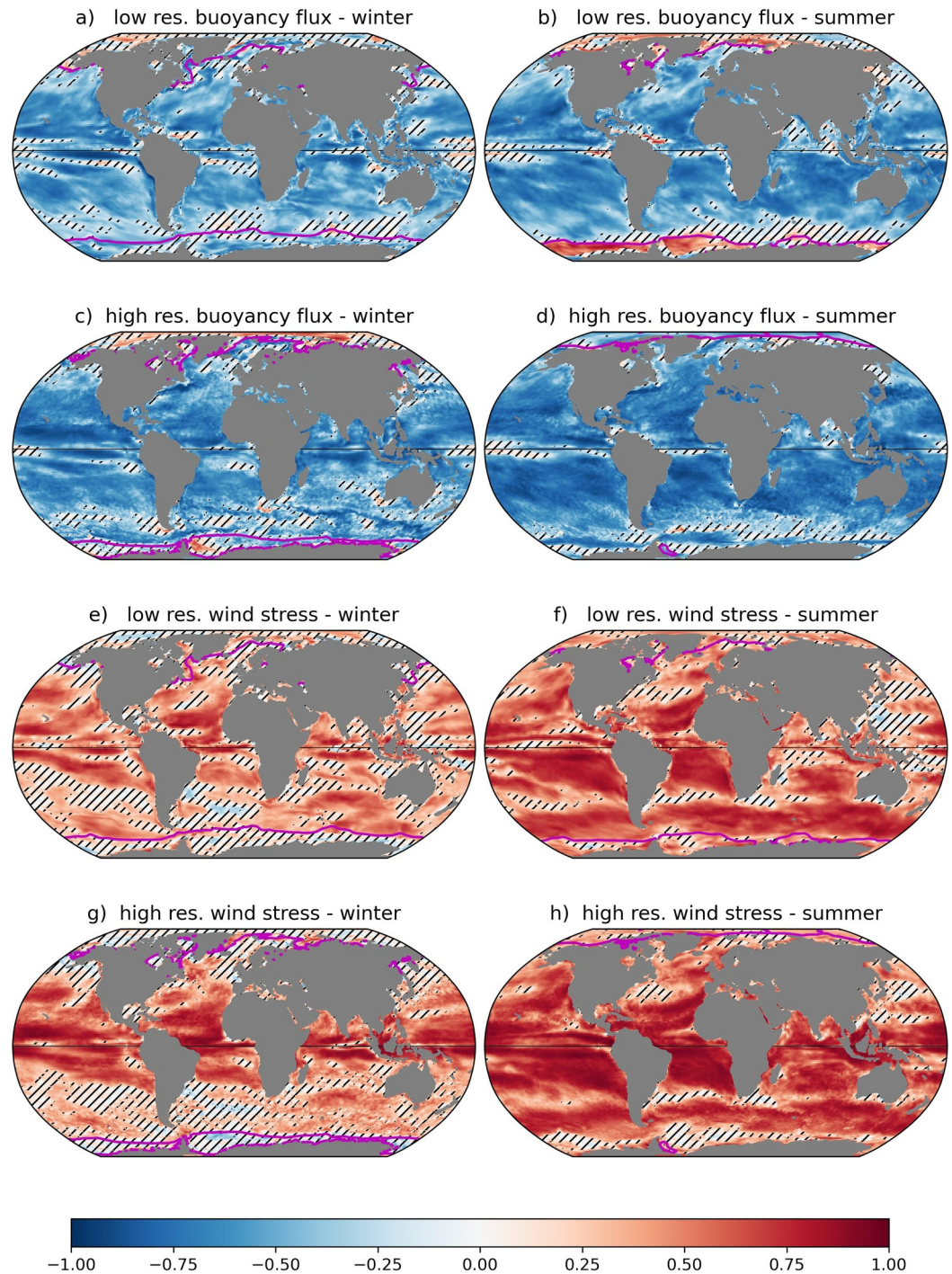


Figure 3. Pearson correlation coefficients of the MLD time series (1970–2018) with the surface forcing fields in the CMCC-NEMO models. (a, b) Low resolution model MLD correlation with the buoyancy flux for winter and summer respectively; (c, d) same fields for the high resolution model. (e, f) MLD correlation with the amplitude of the wind stress for the low resolution model, and (g, h) same fields for the high resolution model. The contour of sea-ice concentration 0.8 is shown in magenta. Areas where the correlations have a p-value lower than 0.1 are hatched. The winter (summer) season is the average over the months of January to March in the Northern (Southern) Hemisphere, and July to September in the Southern (Northern) Hemisphere, respectively.

amplitude for the CMCC models. Their respective correlations with the MLD are shown in Figure 3 for both the low and high resolution model; note that under sea ice the fluxes correspond to ice-ocean interactions, not air-sea interactions. The correlations of MLD with the buoyancy flux are generally negative and correlations with the amplitude of the wind stress are positive, as expected. We do not attempt to disentangle the influence of these two forcings, because they are strongly correlated with one another: the buoyancy flux includes the effects of the latent heat flux and the evaporation, which are both dependent on the wind speed. At low resolution, comparing Figure 3 with the correlations across models, and more specifically the model pairs involving the CMCC model (Figures S5 and S6 in Supporting Information S1) shows that the correlation of MLD with local momentum and thermohaline fluxes is lower than its correlation across models. This suggests that beyond a direct local response to the local air-sea fluxes, the MLD response at interannual time scales is mediated by three-dimensional ocean processes and that these processes seem robust enough to act in very similar fashion in the low resolution models, resulting in very high correlations of the interannual variability of MLD across models (Figure 2). The interannual variability of MLD is less correlated across the different high resolution models (Figures S7 and S8 in Supporting Information S1), because the three dimensional processes are influenced by the resolved mesoscale dynamics.

4. Multi-Decadal Trends of Winds and MLD

The interannual variability of the MLD is similar across the OMIP models: are the multidecadal trends consistent as well, and related to the models' common wind forcing? The first question to consider is whether there are long-term trends of the wind speed in the JRA55-do forcing. Designed to force ocean models, JRA55-do must satisfy various requirements, one of them being that the heat and water budgets must be balanced globally when using observed SST and the OMIP bulk formula to compute the air-sea fluxes. Raw surface variables from atmospheric reanalyses never satisfy this requirement well enough to prevent large drifts in forced ocean model simulations (Griffies et al., 2009). In the process of creating JRA55-do from the raw reanalysis JRA55, Tsujino et al. (2018) noted that major evolutions in the observations that are assimilated in the atmospheric model caused different biases before and after 1973 and 1998, respectively. The correction strategy is thus defined for three different periods: pre 1973 corresponding to the pre-satellite era, 1973–1998, before the advent of the Advanced TIROS Operational Vertical Sounder (ATOVS) and 1998 to present. The winds are corrected by an offset to reduce the bias relative to satellite observations (Tsujino et al., 2018). This strategy, aimed at reducing spurious biases, may also affect observed trends.

Surface wind is a key variable in the climate system and its trends have been studied extensively. It is important to note that the trends depend on the time period over which they are computed. Indeed, Deng et al. (2021), who compared wind speed trends in eight reanalyses, demonstrated that the evolution of wind speed over multiple decades is not well described by a linear trend. For example, over land, a decrease of the wind speed (“terrestrial stilling”) has been documented (e.g., Vautard et al., 2010), but Deng et al. (2021) confirmed that it has reversed since 2010. They analyzed the wind over the oceans in both hemispheres, and found that the increase in the Southern Hemisphere also reversed around 2010. In the Northern Hemisphere, they found no significant trend before 2010, and a decrease afterward. Over the common period over which all data sets were available (1980–2010), JRA55 performed well compared with the other reanalyses (Deng et al., 2021).

The increase in winds over the ocean, especially in the Southern Ocean, has also been documented using satellite observations (Young & Ribal, 2019). We have computed the linear trends of the annual mean wind speed in JRA55-do over the period 1985–2018, using the SciPy library. There are similarities with Young and Ribal (2019), especially with an overall positive trend stronger in the Southern Hemisphere (Figure S11 in Supporting Information S1). However, the amplitude of the trend is underestimated in JRA55-do: $0.09 \text{ m.s}^{-1} \cdot \text{dec}^{-1}$ in JRA55-do between 50°S and 60°S , versus $0.28 \text{ m.s}^{-1} \cdot \text{dec}^{-1}$ in Young and Ribal (2019). A similar underestimation is found in ERA5 (Figure S11 in Supporting Information S1) and other data sets (Deng et al., 2021). Overall, the wind speed trends in JRA55-do are comparable to those of other reanalyses, and thus OMIP seems a good framework to investigate the mixed layer response.

In this section, we choose the period 1970–2018 to study the MLD evolution, for comparison with S21. Trends over this period are shown for JRA55-do (Figures 4a and 4c) and ERA5 (Figures 4b and 4d) for two seasons, demonstrating that the trends in the Southern Ocean are more zonally symmetric and stronger in summer. The comparison of the trends in JRA55-do and ERA5 in Figure 4 reveals similarities and differences, as found by Deng et al. (2021): these details will be discussed in relation with MLD trends later in this section.

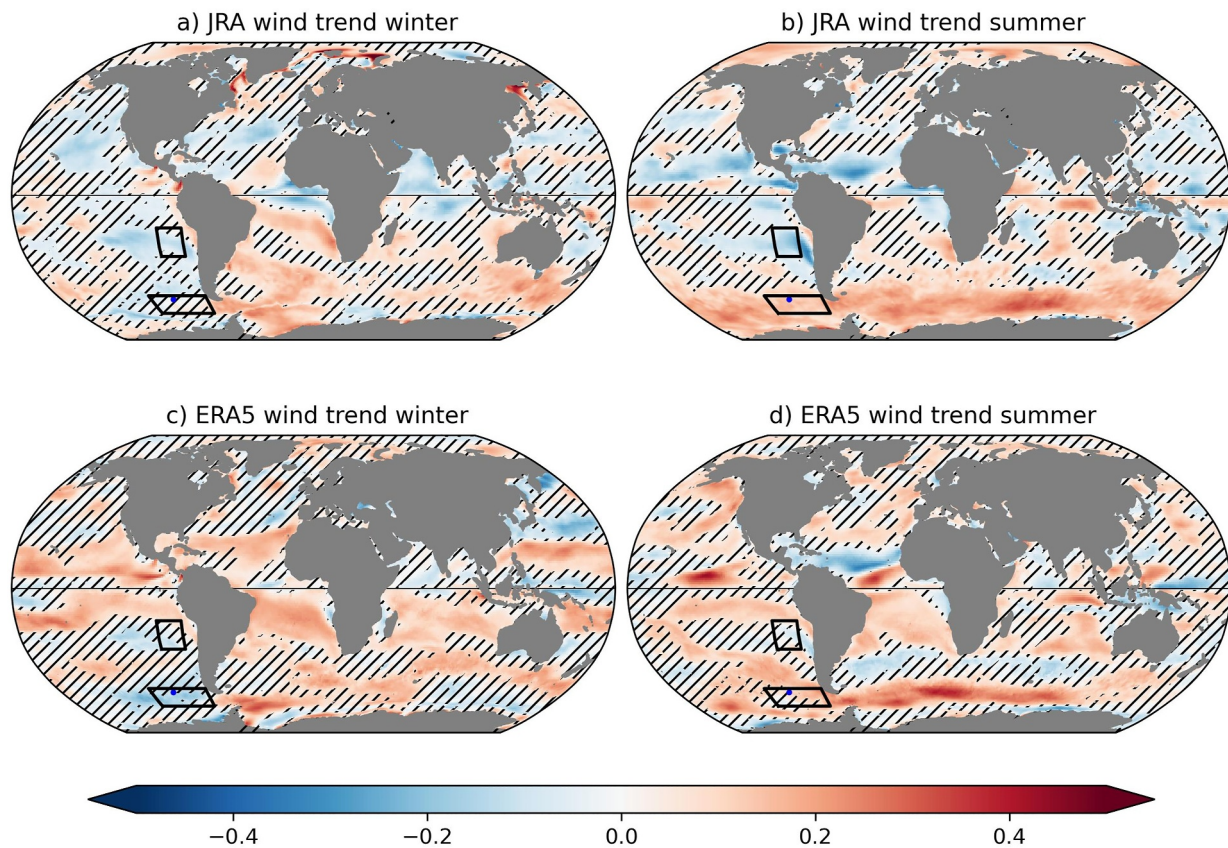


Figure 4. Trends in JRA55-do and ERA5 wind speed, in $\text{m}\cdot\text{s}^{-1}/\text{decade}$. (a, b) Trend of the winter and summer amplitude of the wind speed in JRA55-do over the period 1970–2018. Panels b and d are similar to (a, b), but for ERA5. The two regions used for Figure 6, with contrasted trends in summer, are outlined in black: Southern East Pacific, SEPAC, and East Pacific sector of the Southern Ocean, EPSO. The blue dot in the EPSO region marks the location chosen for the one-dimensional model (100°W , 55°S). The winter (summer) season is the average over the months of January to March in the Northern (Southern) Hemisphere, and July to September in the Southern (Northern) Hemisphere, respectively.

The observed trends of MLD are presented in Figures 5a and 5b. These maps, drawn from Sallées's archived data set (Sallée et al., 2020), are almost identical to S21's Figure 3c for summer trends and to their Extended Data Figure 5c for winter trends. Our different definition of the summer season (July–September in the present paper, vs. August–October in S21) has no noticeable impact. There are large regions where the observed MLD trends are weaker than their standard error, due to the large variability of the MLD: these regions are hatched in Figure 5, following S21. Note that this measure of significance corresponds to a p -value of about 0.3, and thus many of the regions that are not hatched would be considered as having non-significant trends if a more stringent measure were used, such as a lower p -value. S21's main conclusion is that the summer mixed layer has been deepening quasi-globally over the period 1970–2018, at rates ranging from 5 to 10 $\text{m}\cdot\text{dec}^{-1}$ depending on the region (Figure 5b). There are, however, some regions of mixed layer shoaling, for example, the North Central Pacific, which have not been commented upon by S21. Regarding the winter season (Figure 5a), S21 have noted that the trends are less reliable because of the larger interannual variability, and that there is a shoaling of the winter MLD in the Pacific sector of the Southern Ocean that seems significant.

A deepening trend of the mixed layer is also present in the OMIP models in the Southern Ocean in summer, as shown by the multi-model trends in Figures 5d and 5f. This deepening is found in all the models and resolutions (Figures S13 and S15 in Supporting Information S1). It is weaker than observed: the average trend (where significant) in the latitude band 60°S – 50°S is 3.3 m/decade for S21 and 2.1 m/decade for the multi-model mean. IAP-LICOM has a low trend compared with the other models (Figures S13 and S15 in Supporting Information S1) so that the multimodel mean trend is slightly larger if this model is not taken into account (2.5 m/decade), but it is still lower than observed. The difference may be explained by the underestimation of the wind speed trend by JRA55-do (Figure 4; Figure S11 in Supporting Information S1). In the rest of the world, the models do not

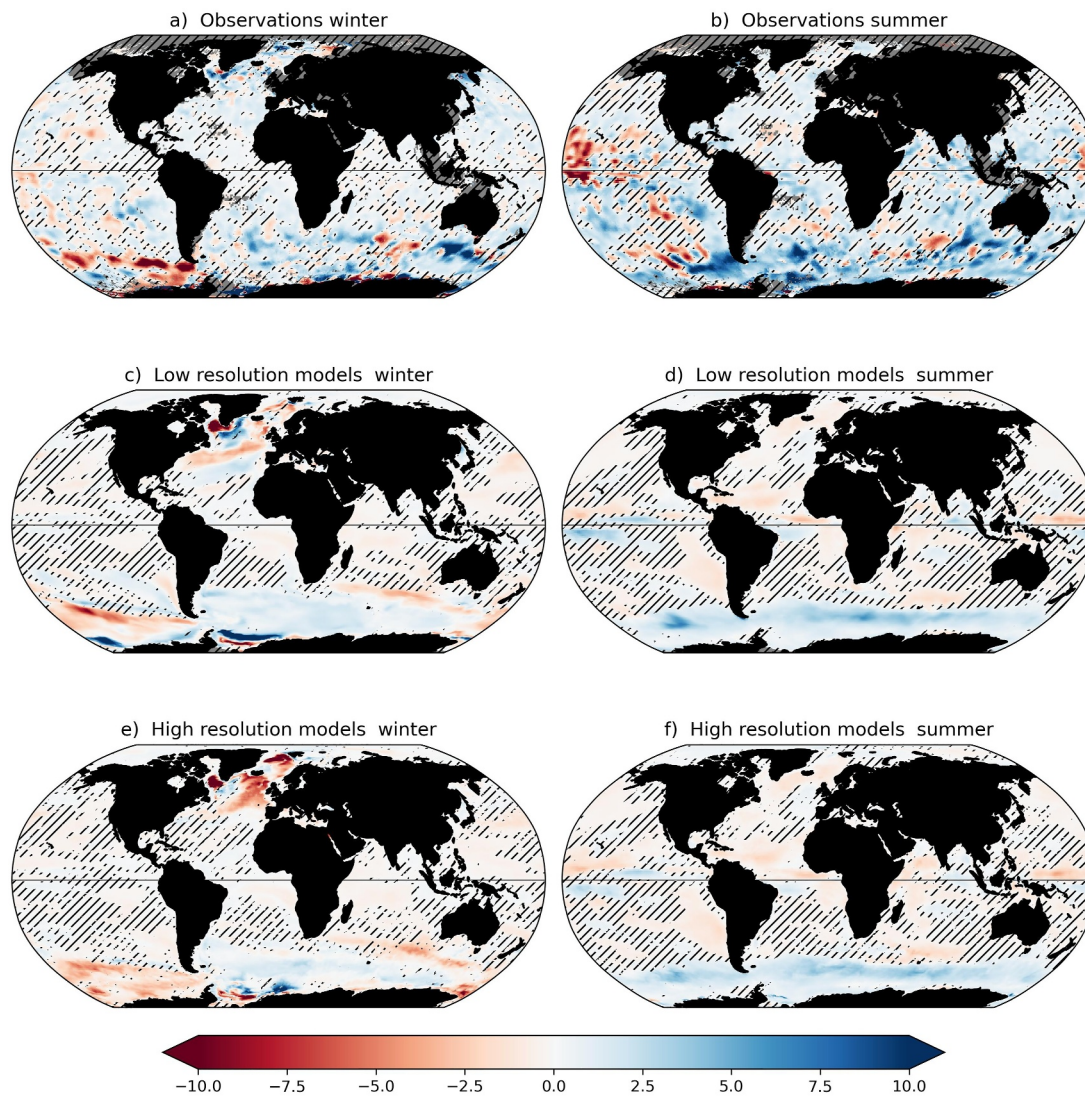


Figure 5. Trends of the MLD over the period 1970–2018 (m/decade). For comparison with S21, blue represents mixed layer deepening, and red mixed layer shoaling. (a, b) Observations from S21. The regions where the standard error of the trend is greater than the trend (condition C1) are hatched. (c, d) Multi-model average of the low resolution models. The regions where condition C1 is satisfied by more than half the models are hatched. (e, f) Same for the high resolution models. The winter (summer) season is the average over the months of January to March in the Northern (Southern) Hemisphere, and July to September in the Southern (Northern) Hemisphere, respectively.

reproduce the summer deepening trends observed by S21. In some cases, such as the Southeast Pacific, the modeled MLD exhibits a shallowing trend that is not found in S21 but is consistent with a weakening trend of the JRA55-do winds, which is absent from ERA5 (Figures 4c and 4d). In other cases, the modeled trends are not significant (some areas in the North Pacific and the Indian Ocean, for example). If the models have a realistic MLD variability, the lower significance of the modeled MLD trends compared to the observed ones could simply result from the underestimated wind trends in JRA55-do. Note that other forcings may also influence MLD trends. We have found significant trends in the buoyancy forcing for the CMCC model in some areas (not shown). However, the pattern of summer trends in the Southern Ocean is not zonally symmetric, unlike the MLD trend. Furthermore, it is positive in the Indian ocean sector, which would make the mixed layer shallower and not deeper. Therefore, in the Southern Ocean in summer, the wind speed seems the main cause of the multidecadal trend in the models.

In winter, the pattern of trends in the Southern Ocean in both models and observations is not zonally symmetric, contrary to the summer season. The models exhibit a shallowing mixed layer trend in the South Pacific sector, a

deepening in the Atlantic sector, and latitude bands of deepening and shallowing south and north of the ACC front in the Indian sector. There is a hint of such a pattern in the JRA55-do winds. For example, the south Pacific mixed layer shoaling of the MLD is also found in observations (Figure 5a) and coincides with a weakening of JRA55-do winds which is also seen in ERA5 (Figures 4a and 4c).

Besides JRA55-do, another forcing set has been used in the framework OMIP. For the first phase OMIP1, the forcing was labeled “CORE” (Griffies et al., 2009). It was based on NCEP and satellite observations and covered the period 1948–2009 (Large & Yeager, 2009). Over the Southern Ocean, positive trends in wind speed are stronger in CORE than in JRA55-do over the period 1970–2009 (Figure S18 in Supporting Information S1). We have evaluated the mixed layer depth trends in three low resolution models run for OMIP1 with CORE forcing (CMCC-NEMO, NCAR-POP and IAP-LICOM). The circumpolar increase of MLD in summer is found in all three models (Figure S19 in Supporting Information S1), IAP-LICOM having a weaker trend, as was the case with OMIP2 forcing. The comparison of both forcings gives us confidence that the summer MLD trend in the Southern Ocean is not specific to JRA55-do-forced models.

Time series are useful to visualize the trends in relation to the interannual variability. Here we show time series in two regions outlined in Figure 4: the East Pacific section of the Southern Ocean (EPSO, from 116°W to 76°W and 63°S to 53°S) and a Southern East Pacific region (SEPAC, from 95°W to 80°W and 32°S to 17°S). These regions are chosen because they exhibit significant, but contrasted MLD trends in summer (Figures 5 and 6): in EPSO, the MLD deepens as observed by S21, but less so (2.1 m/decade vs. 6.7 m/decade). In SEPAC, the MLD shallows in the models (−1 m/decade) but deepens in S21 (3.4 m/decade). Figure 6a, b confirms the good relationship between the MLD and the wind speed for both the interannual variability and the trends. Similar time series covering the whole 53°S–63°S band demonstrate that the EPSO region is representative of the Southern Ocean (Figure S20 in Supporting Information S1). MLD and winds are highly correlated at interannual time scales in both EPSO and SEPAC regions in summer (coefficients of 0.67 and 0.88 respectively; also see Figures 3f and 3h). The multidecadal trends of MLD are consistent with the wind forcing: EPSO shows a significant increase in wind speed (0.13 m.s^{−1}/decade) and SEPAC a significant decrease (−0.14 m.s^{−1}/decade). The relation between MLD and wind speed is complex: this is illustrated by the different patterns of the trends in Figures 4 and 5, and by the fact that the MLD trend in EPSO has almost twice the amplitude of the trend in SEPAC while the wind speed trends have almost the same amplitude. The modeled MLD trend has a sign opposite to the observed trend in the SEPAC region, but we note from Figure 4 that contrary to the JRA55-do forcing, ERA5 has no significant trend there. Multidecadal trends in atmospheric reanalyses are probably not robust in SEPAC, while trends in ERA5 and JRA55-do are similar in other regions, such as EPSO.

A more in-depth investigation of the origin of the mixed layer depth trends would require going beyond the local effect of surface forcing (wind or buoyancy flux). We have already mentioned other processes such as the preconditioning through the advection of water masses, and the eddy fluxes contributing to horizontal advection and restratification. An investigation of all these processes would require budgets of the mixed layer properties, preferably computed online. Alternatively, sensitivity experiments could shed light on the role of different forcing terms (Biastoch et al., 2008). Although global sensitivity simulations are beyond the scope of this manuscript, we have investigated the role of the wind relative to the other atmospheric variables at a single location, using a one-dimensional (1D) model in the vertical dimension. We have set up a version of the NEMO model to simulate the water column at a typical location within the EPSO region (100°W, 55°S, Figure 4), based on the 75-levels configuration developed by Reffray et al. (2015) which uses the same TKE vertical mixing parameterization as CMCC-NEMO. For the simulation mld1d_init, the 1D model is initialized by the solution of the low resolution CMCC-NEMO model at the nearest grid point for the month of December, and run for one year forced by the JRA55-do forcing; the procedure is repeated for each year from 1970 to 2018. A second simulation, mld1d_clim, is initialized with the December climatology of the low resolution CMCC-NEMO, and forced by climatological JRA55-do atmospheric variables with the exception of the winds which retain their variability and differ each year. The original CMCC-NEMO simulation and the two 1D simulations are compared in Figure 6c. At this location, there is a positive trend in wind speed and the MLD increases in summer over the period 1970 to 2018, even though the surface density decreases (not shown). The 1D model reproduces successfully the summer mixed layer depth anomaly every year, although the MLD has a deep bias compared to the full CMCC-NEMO model (the average summer MLD is 76 m in mld1d-init instead of 66 m in CMCC-NEMO). The interannual variability and the multidecadal trend are similar in CMCC-NEMO and mld1d_init (trends are 3.6 m/decade and 3.8 m/decade, respectively). When only the interannual variability of the wind is retained in simulation mld1d_clim, a

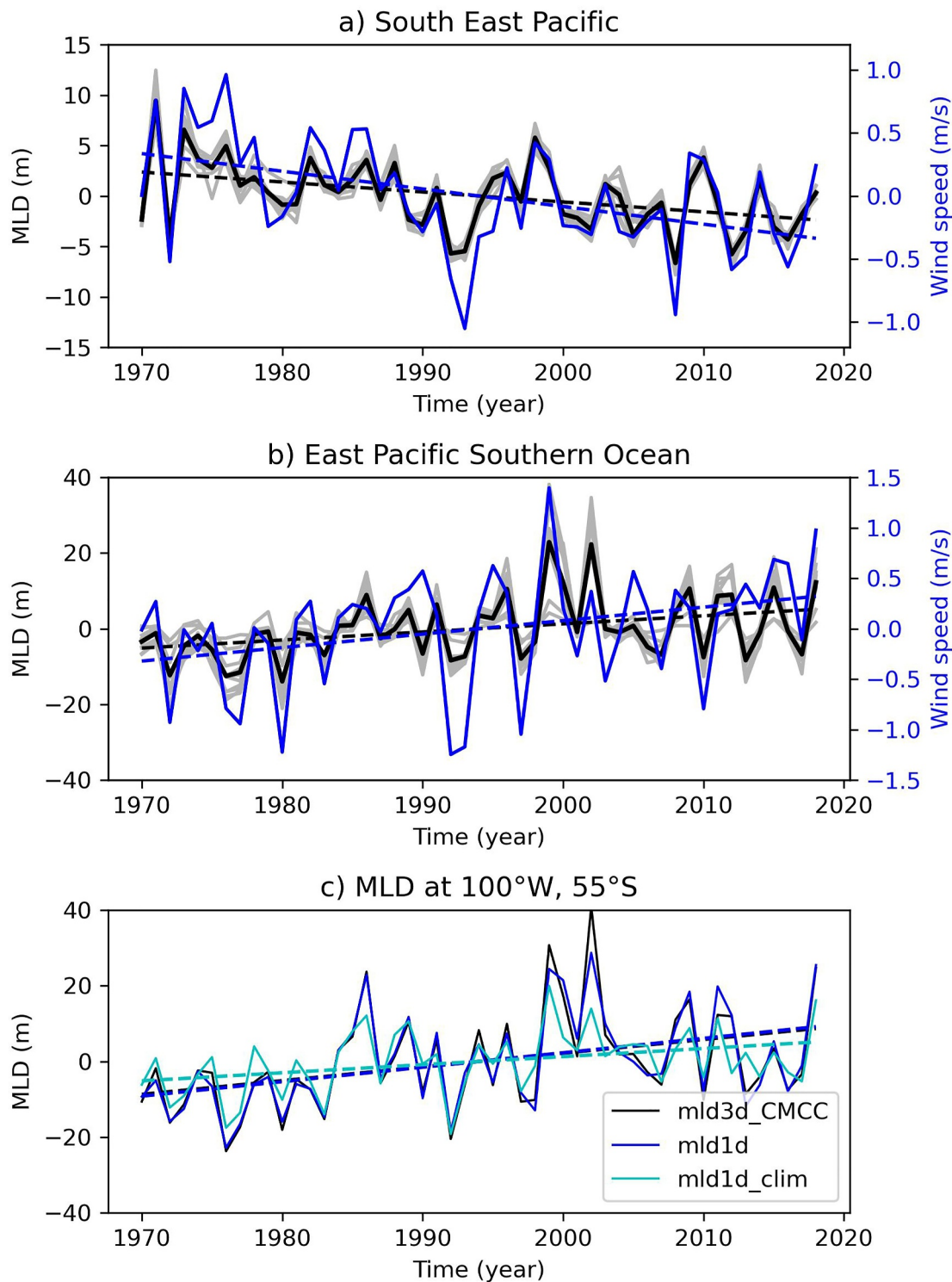


Figure 6. Panels (a, b) time series of model MLD and JRA55-do wind speed anomalies relative to their time-mean, in summer, in the two regions outlined in Figure 4 (Southern East Pacific, SEPAC, and East Pacific sector of the Southern Ocean, EPSO). The gray lines represent each individual model (low and high resolution), and the black line is the multimodel mean (left scale, in m). The blue line is the wind speed (right scale, m/s). A linear trend is indicated for the multimodel mean and the wind speed. Panel (c) time series of MLD anomaly at a grid point in the EPSO region (100°W, 55°S, see Figure 4) for the CMCC-NEMO low resolution model (black line). Two reconstructions of the time series using a one-dimensional NEMO model are also shown (see text).

positive MLD trend remains but it is smaller (2.1 m/decade). Another simulation where only the initial condition is climatological (the forcings being fully varying) exhibits a similar trend (not shown). Thus, the MLD deepening in summer can be reproduced with a 1D model, but the wind changes explain only a part of the trend. The preconditioning, taken into account by initializing the 1D model every year, also plays an important part. Note that the winter time variability is more complex and the trends less significant in the regions considered here, and the variability is not so well reproduced by the 1D model (Figure S16 in Supporting Information S1).

5. Discussion and Conclusion

In OMIP models, the interannual variability of the MLD at spatial scales >100 km is constrained by the atmospheric forcing to a high degree, as demonstrated by the high correlation of the MLD across models. This is true in summer over most of the world's oceans, except for the high resolution models in regions of high mesoscale variability. It is not surprising to find such an impact of the mesoscales, considering that eddies shape the MLD (Gao et al., 2023; Gaube et al., 2019; T23) and that they induce intrinsic interannual variability that is uncorrelated with the atmosphere (Penduff et al., 2018). At multidecadal time scales, the OMIP models reproduce to some extent the deepening trend of the mixed layer observed in the Southern Ocean in summer from 1970 to 2018 (S21), with a zonally symmetric pattern that fits with the strengthening of the wind speed in that region. The lower amplitude of the trend in OMIP compared to observations is probably explained by an underestimation of the wind speed trend in the JRA55-do forcing compared with satellite observations (Young & Ribal, 2019).

S21 suggested that the wind caused a deepening of the mixed layer through local processes: Langmuir circulation, submesoscale frontal instabilities and instabilities of internal wave shears. Some of these processes are parameterized in the OMIP models. Three models include the Fox-Kemper parameterization (Fox-Kemper et al., 2011) to represent restratification by the submesoscale dynamics: the ACCESS-MOM pair and NCAR-POP at low resolution (Table 1). We find that these models do not differ markedly from the others regarding the MLD trends, and thus our results do not point out a key role for this mechanism. Although OMIP models have different biases (T23), they are consistent in their representation of the MLD variability, with the exception of IAP-LICOM which is less correlated with the other models. We conclude that the models' vertical mixing schemes TKE and KPP (Table 1) result in similar representations of MLD variability and trends, while the Canuto scheme (Canuto et al., 2001, 2002) used in IAP-LICOM produces a different variability. The models suggest that the multidecadal MLD trend in the Southern Ocean is in part a simple local response of the MLD to the wind stress, but three dimensional mechanisms involving the ocean circulation cannot be excluded. Using a one-dimensional simulation at a typical location in the Southern Ocean, we have found that the MLD trend of the corresponding three dimensional simulation is fully reproduced only when the 1D model is re-initialized each year by a profile from the 3D simulation. This means that preconditioning during the winter season also plays a part in the summer MLD trends. Buoyancy advection by the meridional Ekman currents is a key process in the Southern Ocean (Rintoul & England, 2002; Sallée et al., 2013). DuVivier et al. (2018) have pointed out the influence of salinity advection by the fronts of the Antarctic Circumpolar Current in the high resolution NCAR-POP model. More recently, Gao et al. (2022) have demonstrated the role of eddy advection in combination with eddy modulation of air-sea fluxes, especially in winter, to determine mixed layer properties in the Southern Ocean. Finally, ocean-ice interaction must also be taken into account.

Outside of the Southern Ocean, S21 claimed that the MLD deepening in summer was quasi-global, despite the fact that their map shows shallowing trends in some areas (Figure 5b). The deepening trend in the OMIP simulations is certainly not global. This is consistent with the fact that the trend in wind speed over the 1970–2018 period is not global in JRA55-do, but rather displays complex spatial patterns of different signs (Figure 4) such as other reanalyses (Deng et al., 2021). This may be a deficiency in the forcing fields, as observations suggest that wind speed trends may be stronger and more globally positive (Young & Ribal, 2019). This calls for updated data sets to force ocean models for the next phase of OMIP.

The study of mixed layer depth trends from observations should be carried out jointly with an analysis of the trends in wind speeds. This was attempted in a recent study (Roch et al., 2023) focused on the recent years when profiles of the ARGO observing network are available (2006–2021). OMIP models are run only up to 2018, but we computed the trends over the period 2006–2018 (Figure S17 in Supporting Information S1) to compare. The models show complex patterns of shallowing (e.g., in the Equatorial Pacific) and deepening (e.g., in the Southern

Ocean in summer), very different from the more widespread deepening shown by Roch et al. (2023). We assume that the trends in Roch et al. (2023) are very dependent on the method they have used to remove the effects of the El-Niño Southern Ocean Oscillation (ENSO). Over such a short 15-years period the variability is very much influenced by ENSO, and the changes in MLD or winds cannot be described by a simple linear trend. We thus argue that the conclusion of Roch et al. (namely, that trends in MLD over the ARGO period are not related to trends of the wind speed) is not definitive and that a longer period is required to evaluate trends.

Considering the sparseness of in-situ observations before the ARGO period, we suspect that the analysis of S21 also depends on the method to some degree, because their computed trends are not consistent with other studies in some areas. A shallowing of the mixed layer in winter is observed in the Kuroshio region (141°E–155°E, 30°N–37°N) over the period 1960–2021 (Sugimoto, 2022), at a rate of 4.75 m/decade. The OMIP models reproduce a shallowing, although weaker (2 m/decade), while in the S21 data set the winter mixed layer deepens in that region by 7.7 m/decade. The difference between the two observation-based studies can be explained by the fact that they do not use the same observations. In the work of Sugimoto (2022), the MLD is determined using a temperature threshold, which is appropriate for this region, while S21 uses a density threshold which is more robust across the world ocean in theory, but requires knowledge of both temperature and salinity. Before the ARGO period, temperature profiles are more numerous than profiles where both temperature and salinity have been measured. Our hypothesis is thus that S21's winter mixed layer deepening in the Kuroshio region is spurious and that the significance of S21's trend is overestimated in that region, and possibly elsewhere.

In the present analysis, we have considered only the mixed layer depth and the air-sea fluxes, and we have focused on summer trends. The winter trends are more diverse across models and less significant than the summer trends. A more in-depth exploration of their origin is beyond the scope of this paper. This will require taking into account the representation of the underlying stratification and of the circulation by the different models. Furthermore, we expect that the processes responsible for the winter trends differ in different regions of the world ocean.

Overall, our analysis demonstrates the good capacity of the OMIP models to simulate the multidecadal trends of the mixed layer depth, and confirms that positive trends in wind speed can cause widespread MLD deepening in summer. More significant trends are expected to develop in the coming decades, as the Earth continues to warm. The eddy-rich models developed as part of HighResMIP will be necessary to assess the significance of the projected trends in the presence of a realistic background variability in the surface mixed layer.

Data Availability Statement

The following OMIP model output, published on the Earth System Grid Federation (ESGF), has been used: ACCESS-OM2 (Hayashida et al., 2021), CESM2 (Danabasoglu, 2019), CMCC-CM2-SR5 (Fogli et al., 2020), FGOALS-f3-H (Lin, 2020), FGOALS-f3-L (Lin, 2019). The 0.1° ACCESS-MOM data is available from <http://dx.doi.org/10.25914/608097cb3433f>, (Kiss et al., 2022). The data used to produce the figures and the corresponding Python notebook are archived on Zenodo at <https://doi.org/10.5281/zenodo.15004986> (Treguier, 2025).

References

- Alexander, M. A., Scott, J. D., Friedland, K. D., Mills, K. E., Nye, J. A., Pershing, A. J., & Thomas, A. C. (2018). Projected sea surface temperatures over the 21st century: Changes in the mean, variability and extremes for large marine ecosystem regions of Northern Oceans. *Elementa: Science of the Anthropocene*, 6, 9. <https://doi.org/10.1525/elementa.191>
- Belcher, S. E., Grant, A. L. M., Hanley, K. E., Fox-Kemper, B., Van Roekel, L., Sullivan, P. P., et al. (2012). A global perspective on Langmuir turbulence in the ocean surface boundary layer. *Geophysical Research Letters*, 39(18), L18605. <https://doi.org/10.1029/2012GL052932>
- Bjastoch, A., Böning, C. W., Getzlaff, J., Molines, J.-M., & Madec, G. (2008). Causes of interannual–decadal variability in the meridional overturning circulation of the midlatitude North Atlantic Ocean. *Journal of Climate*, 21(24), 6599–6615. <https://doi.org/10.1175/2008JCLI2404.1>
- Bindoff, N. L., Cheung, W. W. L., Kairo, J. G., Aristegui, J., Guinder, V. A., Hallberg, R., et al. (2019). Changing ocean, marine ecosystems, and dependent communities. In H. O. Pörtner, D. C. Roberts, V. Masson-Delmotte, P. Zhai, M. Tignor, E. Poloczanska, et al. (Eds.), *IPCC Special Report on the Ocean and Cryosphere in a Changing Climate* (pp. 447–586). Cambridge University Press. <https://doi.org/10.1017/9781009157964.007>
- Blanke, B., & Delecluse, P. (1993). Variability of the Tropical Atlantic Ocean simulated by a general circulation model with two different mixed-layer physics. *Journal of Physical Oceanography*, 23(7), 1363–1388. [https://doi.org/10.1175/1520-0485\(1993\)023<1363:VOTTAO>2.0.CO;2](https://doi.org/10.1175/1520-0485(1993)023<1363:VOTTAO>2.0.CO;2)
- Canuto, V. M., Howard, A., Cheng, Y., & Dubovikov, M. S. (2001). Ocean turbulence. Part I: One-point closure model—Momentum and heat vertical diffusivities. *Journal of Physical Oceanography*, 31(6), 1413–1426. [https://doi.org/10.1175/1520-0485\(2001\)031<1413:OTPIOP>2.0.CO;2](https://doi.org/10.1175/1520-0485(2001)031<1413:OTPIOP>2.0.CO;2)

Acknowledgments

This work is a contribution to the Mixed Layer hEterogeneity (MEDLEY) project. MEDLEY has received funding from the Joint Programming Initiative (JPI) Climate and JPI Oceans programs under the 2019 joint call, managed by the French Agence Nationale de la Recherche (contract no. 19-JPOC-0001-01). AEK is supported by the Australian Research Council Grant LP200100406. ACCESS-MOM data was provided by the Consortium for Ocean-Sea Ice Modelling in Australia (COSIMA) (<http://www.cosima.org.au>) using computational resources provided by the Australian Government through the National Computational Infrastructure (NCI) under the National Computational Merit Allocation Scheme and ANU Merit Allocation Scheme. SGY acknowledges support from award NA24OARX431G0043 of NOAA's Climate Variability and Predictability program. The National Center for Atmospheric Research (NCAR) is a major facility sponsored by the National Science Foundation (NSF) under Cooperative Agreement 1852977.

- Canuto, V. M., Howard, A., Cheng, Y., & Dubovikov, M. S. (2002). Ocean turbulence. Part II: Vertical diffusivities of momentum, heat, salt, mass, and passive scalars. *Journal of Physical Oceanography*, 32(1), 240–264. [https://doi.org/10.1175/1520-0485\(2002\)032<0240:OTPIVD>2.0.CO;2](https://doi.org/10.1175/1520-0485(2002)032<0240:OTPIVD>2.0.CO;2)
- Chassignet, E. P., Smith, L. T., Halliwell, G. R., & Bleck, R. (2003). North Atlantic simulations with the Hybrid Coordinate Ocean Model (HYCOM): Impact of the vertical coordinate choice, reference pressure, and thermobaricity. *Journal of Physical Oceanography*, 33(12), 2504–2526. [https://doi.org/10.1175/1520-0485\(2003\)033<2504:NASWTH>2.0.CO;2](https://doi.org/10.1175/1520-0485(2003)033<2504:NASWTH>2.0.CO;2)
- Chassignet, E. P., Yeager, S. G., Fox-Kemper, B., Bozec, A., Castruccio, F., Danabasoglu, G., et al. (2020). Impact of horizontal resolution on global ocean–sea ice model simulations based on the experimental protocols of the Ocean Model Intercomparison Project Phase 2 (OMIP-2). *Geoscientific Model Development*, 13(9), 4595–4637. <https://doi.org/10.5194/gmd-13-4595-2020>
- Danabasoglu, G. (2019). NCAR CESM2 model output prepared for CMIP6 OMIP omip1. *Earth System Grid Federation*. <https://doi.org/10.22033/ESGF/CMIP6.7678>
- Danabasoglu, G., Lamarque, J.-F., Bacmeister, J., Bailey, D. A., DuVivier, A. K., Edwards, J., et al. (2020). The Community Earth System Model Version 2 (CESM2). *Journal of Advances in Modeling Earth Systems*, 12(2), e2019MS001916. <https://doi.org/10.1029/2019MS001916>
- D'Asaro, E. A. (2014). Turbulence in the upper-ocean mixed layer. *Annual Review of Marine Science*, 6(1), 101–115. <https://doi.org/10.1146/annurev-marine-010213-135138>
- de Boyer Montégut, C., Madec, G., Fisher, A. S., Lazar, A., & Iudicone, D. (2004). Mixed layer depth over the global ocean: An examination of profile data and a profile-based climatology. *Journal of Geophysical Research*, 109(C12), C12003. <https://doi.org/10.1029/2004JC002378>
- Deng, K., Azorin-Molina, C., Minola, L., Zhang, G., & Chen, D. (2021). Global near-surface wind speed changes over the last decades revealed by reanalyses and CMIP6 model simulations. *Journal of Climate*, 34(6), 2219–2234. <https://doi.org/10.1175/JCLI-D-20-0310.1>
- DuVivier, A. K., Large, W. G., & Small, R. J. (2018). Argo observations of the deep mixing band in the southern ocean: A salinity modeling challenge. *Journal of Geophysical Research: Oceans*, 123(10), 7599–7617. <https://doi.org/10.1029/2018JC014275>
- Fogli, P. G., Iovino, D., & Lovato, T. (2020). CMCC CMCC-CM2-SR5 model output prepared for CMIP6 OMIP omip1. *Earth System Grid Federation*. <https://doi.org/10.22033/ESGF/CMIP6.13230>
- Fox-Kemper, B., Danabasoglu, G., Ferrari, R., Griffies, S. M., Hallberg, R. W., Holland, M. M., et al. (2011). Parameterization of mixed layer eddies. III: Implementation and impact in global ocean climate simulations. *Modelling and Understanding the Ocean Mesoscale and Sub-mesoscale*, 39(1), 61–78. <https://doi.org/10.1016/j.ocemod.2010.09.002>
- Fox-Kemper, B., Ferrari, R., & Hallberg, R. (2008). Parameterization of mixed layer eddies. Part I: Theory and diagnosis. *Journal of Physical Oceanography*, 38(6), 1145–1165. <https://doi.org/10.1175/2007JPO3792.1>
- Fox-Kemper, B., Hewitt, H. T., Xiao, C., Aðalgeirsdóttir, G., Drijfhout, S. S., Edwards, T. L., et al. (2021). Ocean, cryosphere and sea level change. In V. Masson-Delmotte, P. Zhai, A. Pirani, S. L. Connors, C. Péan, S. Berger, et al. (Eds.), *Climate Change 2021: The Physical Science Basis. Contribution of Working Group I to the Sixth Assessment Report of the Intergovernmental Panel on Climate Change* (pp. 1211–1361). Cambridge University Press. <https://doi.org/10.1017/9781009157896.011>
- Gaillard, F., Reynaud, T., Thierry, V., Kolodziejczyk, N., & von Schuckmann, K. (2016). In situ–based reanalysis of the global ocean temperature and salinity with ISAS: Variability of the heat content and steric height. *Journal of Climate*, 29(4), 1305–1323. <https://doi.org/10.1175/JCLI-D-15-0028.1>
- Gao, Y., Kamenkovich, I., & Perlin, N. (2023). Origins of mesoscale mixed-layer depth variability in the Southern Ocean. *Ocean Science*, 19(3), 615–627. <https://doi.org/10.5194/os-19-615-2023>
- Gao, Y., Kamenkovich, I., Perlin, N., & Kirtman, B. (2022). Oceanic advection controls mesoscale mixed layer heat budget and air–sea heat exchange in the Southern Ocean. *Journal of Physical Oceanography*, 52(4), 537–555. <https://doi.org/10.1175/JPO-D-21-0063.1>
- Gaube, P., McGillicuddy, J., Jr., & Moulin, A. J. (2019). Mesoscale eddies modulate mixed layer depth globally. *Geophysical Research Letters*, 46(3), 1505–1512. <https://doi.org/10.1029/2018GL080006>
- Gillard, L. C., Pennelly, C., Johnson, H. L., & Myers, P. G. (2022). The effects of atmospheric and lateral buoyancy fluxes on Labrador Sea mixed layer depth. *Ocean Modelling*, 171, 101974. <https://doi.org/10.1016/j.ocemod.2022.101974>
- Griffies. (2012). *Elements of the Modular Ocean Model (MOM) (2012 release with updates) (GFDL Ocean Group Technical Report 7)* (p. 632). NOAA/Geophysical Fluid Dynamics Laboratory. Retrieved from https://mom-ocean.github.io/assets/pdfs/MOM5_manual.pdf
- Griffies, S. M., Biastoch, A., Böning, C., Bryan, F., Danabasoglu, G., Chassignet, E. P., et al. (2009). Coordinated Ocean-Ice Reference Experiments (COREs). *Ocean Modelling*, 26(1–2), 1–46. <https://doi.org/10.1016/j.ocemod.2008.08.007>
- Griffies, S. M., Danabasoglu, G., Durack, P. J., Adcroft, A. J., Balaji, V., Böning, C. W., et al. (2016). OMIP contribution to CMIP6: Experimental and diagnostic protocol for the physical component of the Ocean Model Intercomparison Project. *Geoscientific Model Development*, 9(9), 3231–3296. <https://doi.org/10.5194/gmd-9-3231-2016>
- Gulev, S. K., Thorne, P. W., Ahn, J., Dentener, F. J., Domingues, C. M., Gerland, S., et al. (2021). Changing state of the climate system. In V. Masson-Delmotte, P. Zhai, A. Pirani, S. L. Connors, C. Péan, S. Berger, et al. (Eds.), *Climate Change 2021: The Physical Science Basis. Contribution of Working Group I to the Sixth Assessment Report of the Intergovernmental Panel on Climate Change* (pp. 287–422). Cambridge University Press. <https://doi.org/10.1017/9781009157896.004>
- Hallberg, R. (2013). Using a resolution function to regulate parameterizations of oceanic mesoscale eddy effects. *Ocean Modelling*, 72, 92–103. <https://doi.org/10.1016/j.ocemod.2013.08.007>
- Hayashida, H., Kiss, A., Hogg, A., Hannah, N., Dias, F. B., Brassington, G., et al. (2021). CSIRO-COSIMA ACCESS-OM2 model output prepared for CMIP6 OMIP omip2. *Earth System Grid Federation*. <https://doi.org/10.22033/ESGF/CMIP6.14689>
- Heuzé, C. (2021). Antarctic bottom water and North Atlantic deep water in CMIP6 models. *Ocean Science*, 17(1), 59–90. <https://doi.org/10.5194/os-17-59-2021>
- Holte, J., Talley, L. D., Gilson, J., & Roemmich, D. (2017). An Argo mixed layer climatology and database. *Geophysical Research Letters*, 44(11), 5618–5626. <https://doi.org/10.1002/2017GL073426>
- Iovino, D., Masina, S., Storto, A., Cipollone, A., & Stepanov, V. N. (2016). A 1/16degree eddying simulation of the global NEMO sea-ice–ocean system. *Geoscientific Model Development*, 9(8), 2665–2684. <https://doi.org/10.5194/gmd-9-2665-2016>
- Kiss, A. E., Hogg, A. M. C., Hannah, N., Boeira Dias, F., Brassington, G. B., Chamberlain, M. A., et al. (2020). ACCESS-OM2 v1.0: A global ocean sea ice model at three resolutions. *Geoscientific Model Development*, 13(2), 401–442. <https://doi.org/10.5194/gmd-13-401-2020>
- Kiss, A. E., Hogg, A. M. C., Hannah, N., Boeira Dias, F., Brassington, G. B., Chamberlain, M. A., et al. (2022). ACCESS-OM2 0.1 degree global model output (interannual forcing simulation) [Dataset]. *Nuevos Catálogos Industrial & Electrónica*. <https://doi.org/10.25914/608097cb3433f>
- Large, W. G., McWilliams, J. C., & Doney, S. C. (1994). Oceanic vertical mixing: A review and a model with a nonlocal boundary layer parameterization. *Reviews of Geophysics*, 32(4), 363–403. <https://doi.org/10.1029/94RG01872>
- Large, W. G., & Yeager, S. G. (2009). The global climatology of an interannually varying air–sea flux data set. *Climate Dynamics*, 33(2), 341–364. <https://doi.org/10.1007/s00382-008-0441-3>

- Li, L., Yu, Y., Tang, Y., Lin, P., Xie, J., Song, M., et al. (2020). The Flexible Global Ocean-Atmosphere-Land System Model Grid-Point Version 3 (FGOALS-g3): Description and evaluation. *Journal of Advances in Modeling Earth Systems*, 12(9), e2019MS002012. <https://doi.org/10.1029/2019MS002012>
- Li, Q., & Lee, S. (2017). A mechanism of mixed layer formation in the Indo–Western Pacific Southern Ocean: Preconditioning by an eddy-driven jet-scale overturning circulation. *Journal of Physical Oceanography*, 47(11), 2755–2772. <https://doi.org/10.1175/JPO-D-17-0006.1>
- Li, Q., Webb, A., Fox-Kemper, B., Craig, A., Danabasoglu, G., Large, W. G., & Vertenstein, M. (2016). Langmuir mixing effects on global climate: WAVEWATCH III in CESM. *Waves and Coastal, Regional and Global Processes*, 103, 145–160. <https://doi.org/10.1016/j.ocemod.2015.07.020>
- Lin, P. (2019). CAS FGOALS-f3-L model output prepared for CMIP6 OMIP omip1. *Earth System Grid Federation*. <https://doi.org/10.22033/ESGF/CMIP6.3413>
- Lin, P. (2020). CAS FGOALS-f3-H model output prepared for CMIP6 OMIP omip2. *Earth System Grid Federation*. <https://doi.org/10.22033/ESGF/CMIP6.13283>
- Lin, P., Yu, Z., Liu, H., Yu, Y., Li, Y., Jiang, J., et al. (2020). LICOM model datasets for the CMIP6 Ocean model intercomparison project. *Advances in Atmospheric Sciences*, 37(3), 239–249. <https://doi.org/10.1007/s00376-019-9208-5>
- Llort, J., Lévy, M., Sallée, J. B., & Tagliabue, A. (2019). Nonmonotonic response of primary production and export to changes in mixed-layer depth in the Southern Ocean. *Geophysical Research Letters*, 46(6), 3368–3377. <https://doi.org/10.1029/2018GL081788>
- Madec, G., & the NEMO team. (2016). *NEMO reference manual 3_6_STABLE* (Vol. 27). Institut Pierre-Simon Laplace (IPSL).
- Marshall, J., & Schott, F. (1999). Open-ocean convection: Observations, theory, and models. *Reviews of Geophysics*, 37, 1–64. <https://doi.org/10.1029/98rg02739>
- Penduff, T., Sérazin, G., Leroux, S., Close, S., Molines, J.-M., Barnier, B., et al. (2018). Chaotic variability of ocean heat content: Climate-relevant features and observational implications. *Oceanography*, 31(2). <https://doi.org/10.5670/oceanog.2018.210>
- Reffray, G., Bourdalle-Badie, R., & Calone, C. (2015). Modelling turbulent vertical mixing sensitivity using a 1-D version of NEMO. *Geoscientific Model Development*, 8(1), 69–86. <https://doi.org/10.5194/gmd-8-69-2015>
- Rintoul, S. R., & England, M. H. (2002). Ekman transport dominates local air–sea fluxes in driving variability of subtropical mode water. *Journal of Physical Oceanography*, 32(5), 1308–1321. [https://doi.org/10.1175/1520-0485\(2002\)032<1308:ETDLAS>2.0.CO;2](https://doi.org/10.1175/1520-0485(2002)032<1308:ETDLAS>2.0.CO;2)
- Roch, M., Brandt, P., & Schmidt, S. (2023). Recent large-scale mixed layer and vertical stratification maxima changes. *Frontiers in Marine Science*, 10. <https://doi.org/10.3389/fmars.2023.1277316>
- Rudzin, J. E., Shay, L. K., & Johns, W. E. (2018). The influence of the barrier layer on SST response during tropical cyclone wind forcing using idealized experiments. *Journal of Physical Oceanography*, 48(7), 1471–1478. <https://doi.org/10.1175/JPO-D-17-0279.1>
- Sallée, J.-B., Pellichero, V., Akhondas, C., Pauthenet, E., Vignes, L., Schmidt, S., et al. (2021). Summertime increases in upper-ocean stratification and mixed-layer depth. *Nature*, 591(7851), 592–598. <https://doi.org/10.1038/s41586-021-03303-x>
- Sallée, J.-B., Pellichero, V., Akhondas, C., Pauthenet, E., Vignes, L., Schmidt, S., et al. (2020). Fifty-year changes of the world ocean's surface layer in response to climate change [Dataset]. *Zenodo*. <https://doi.org/10.5281/zenodo.5776180>
- Sallée, J.-B., Shuckburgh, E., Bruneau, N., Meijers, A. J. S., Bracegirdle, T. J., & Wang, Z. (2013). Assessment of Southern Ocean mixed-layer depths in CMIP5 models: Historical bias and forcing response. *Journal of Geophysical Research: Oceans*, 118(4), 1845–1862. <https://doi.org/10.1002/jgrc.20157>
- Sein, D. V., Koldunov, N. V., Danilov, S., Sidorenko, D., Wekerle, C., Cabos, W., et al. (2018). The relative influence of atmospheric and oceanic model resolution on the circulation of the North Atlantic Ocean in a coupled climate model. *Journal of Advances in Modeling Earth Systems*, 10(8), 2026–2041. <https://doi.org/10.1029/2018MS001327>
- Sérazin, G., Tréguier, A. M., & de Boyer Montégut, C. (2023). A seasonal climatology of the upper ocean pycnocline. *Frontiers in Marine Science*, 10. <https://doi.org/10.3389/fmars.2023.1120112>
- Smith, R., Jones, P. W., Briegleb, P. A., Bryan, O., Danabasoglu, G., Dennis, M. L., et al. (2010). *The Parallel Ocean Program (POP) reference manual: Ocean component of the Community Climate System Model (CCSM) (LAUR-10-01853)* (p. 140). UCAR/NCAR.
- Somavilla, R., González-Pola, C., & Fernández-Díaz, J. (2017). The warmer the ocean surface, the shallower the mixed layer. How much of this is true? *Journal of Geophysical Research: Oceans*, 122(9), 7698–7716. <https://doi.org/10.1002/2017JC013125>
- Sugimoto, S. (2022). Decreasing wintertime mixed-layer depth in the northwestern North Pacific subtropical gyre. *Geophysical Research Letters*, 49(2), e2021GL095091. <https://doi.org/10.1029/2021GL095091>
- Treguier, A. M. (2025). Multidecadal trends of the mixed layer depth and their relation to the wind in global ocean models forced by an atmospheric reanalysis: Supporting data (submitted version) [Dataset]. *Zenodo*. <https://doi.org/10.5281/zenodo.15004987>
- Treguier, A. M., de Boyer Montégut, C., Bozec, A., Chassignet, E. P., Fox-Kemper, B., McC. Hogg, A., et al. (2023). The mixed-layer depth in the Ocean Model Intercomparison Project (OMIP): Impact of resolving mesoscale eddies. *Geoscientific Model Development*, 16(13), 3849–3872. <https://doi.org/10.5194/gmd-16-3849-2023>
- Tsujino, H., Urakawa, L. S., Griffies, S. M., Danabasoglu, G., Adcroft, A. J., Amaral, A. E., et al. (2020). Evaluation of global ocean–sea-ice model simulations based on the experimental protocols of the Ocean Model Intercomparison Project phase 2 (OMIP-2). *Geoscientific Model Development*, 13(8), 3643–3708. <https://doi.org/10.5194/gmd-13-3643-2020>
- Tsujino, H., Urakawa, S., Nakano, H., Small, R. J., Kim, W. M., Yeager, S. G., et al. (2018). JRA-55 based surface dataset for driving ocean–sea-ice models (JRA55-do). *Ocean Modelling*, 130, 79–139. <https://doi.org/10.1016/j.ocemod.2018.07.002>
- Vautard, R., Cattiaux, J., Yiou, P., Thépaut, J.-N., & Ciais, P. (2010). Northern Hemisphere atmospheric stilling partly attributed to an increase in surface roughness. *Nature Geoscience*, 3(11), 756–761. <https://doi.org/10.1038/ngeo979>
- von Schuckmann, K., Cheng, L., Palmer, M. D., Hansen, J., Tassone, C., Aich, V., et al. (2020). Heat stored in the Earth system: Where does the energy go? *Earth System Science Data*, 12(3), 2013–2041. <https://doi.org/10.5194/essd-12-2013-2020>
- Wang, Q., Danilov, S., Sidorenko, D., Timmermann, R., Wekerle, C., Wang, X., et al. (2014). The Finite Element Sea Ice-Ocean Model (FESOM) v.1.4: Formulation of an ocean general circulation model. *Geoscientific Model Development*, 7(2), 663–693. <https://doi.org/10.5194/gmd-7-663-2014>
- Willebrand, J., Barnier, B., Böning, C., Dieterich, C., Killworth, P. D., Le Provost, C., et al. (2001). Circulation characteristics in three eddy-permitting models of the North Atlantic. *Dynamics of the North Atlantic Circulation: Simulation and Assimilation with High-Resolution Models (DYNAMO)*, 48(2), 123–161. [https://doi.org/10.1016/S0079-6611\(01\)00003-9](https://doi.org/10.1016/S0079-6611(01)00003-9)
- Yamaguchi, R., & Suga, T. (2019). Trend and variability in global upper-ocean stratification since the 1960s. *Journal of Geophysical Research: Oceans*, 124(12), 8933–8948. <https://doi.org/10.1029/2019JC015439>
- Young, I. R., & Ribal, A. (2019). Multiplatform evaluation of global trends in wind speed and wave height. *Science*, 364(6440), 548–552. <https://doi.org/10.1126/science.aav9527>